Carbohydrate Polymers 83 (2011) 438–446

Contents lists available at ScienceDirect

Carbohydrate Polymers

journal homepage: www.elsevier.com/locate/carbpol

Synthesis and characterization of chitosan and silver loaded chitosan nanoparticles for bioactive polyester

S. Wazed Ali [a], S. Rajendran [b], Mangala Joshi [a,*]

[a] Department of Textile Technology, Indian Institute of Technology, New Delhi, Hauz Khas, 110016, India
[b] Institute for Materials Research and Innovation, The University of Bolton, Bolton, BL3 5AB, United Kingdom

ARTICLE INFO

Article history:
Received 21 May 2010
Received in revised form 21 July 2010
Accepted 2 August 2010
Available online 11 August 2010

Keywords:
Chitosan nanoparticles
Silver loaded chitosan nanoparticles
TEM
MIC
Polyester
Bioactivity

ABSTRACT

The paper focuses on the synthesis of chitosan nanoparticles (CSN) by ionic gelation with sodium tripolyphosphate and subsequently its loading with silver ions to produce silver loaded chitosan nanoparticles (Ag-CSN). The aim was to enhance the antibacterial property of chitosan in the nanoparticle form and thus improve its bactericidal efficacy when applied on polyester fabrics. The average particle size of CSN and Ag-CSN was 115 nm and 165 nm, respectively. The structure of CSN and Ag-CSN was studied by XRD, FTIR, DSC, TGA and TEM analysis. The minimum inhibitory concentration of both the CSN and Ag-CSN against *Staphylococcus aureus* bacteria was found to be 50 and 500 times less, respectively, as compared to bulk chitosan. Silver loading on the synthesized CSN showed synergistic antimicrobial effect against *S. aureus* bacteria. The release of Ag^+ from Ag-CSN finished polyester fabric is substantiated by antibacterial testing which shows a clear zone of inhibition.

1. Introduction

The textile materials have generated a considerable interest in the medical field where these wide range of materials in the form of monofilament, multifilament, woven or nonwoven structures are being used as sutures, bandages, scaffolds, wound dressing, masks, surgical gowns and hospital linen, etc. A lot of commercial medical textile products are available with antimicrobial property wherein the growth of micro-organisms is controlled by treatment with antimicrobial agents. Antimicrobial agents can also be integrated in textiles substrates to make these rot proof, mildew stain proof and to prevent perspiration odor resulting from microbial growth on textiles.

The major classes of synthetic antimicrobial agents for textiles include triclosan, metal and their salts, organometallics, phenols, quaternary ammonium compounds and organosilicons, etc. (Purwar & Joshi, 2004). But these chemicals would often yield highly toxic or otherwise undesirable by-products. In view of these environmental and ecological concerns and the lack of alternatives that meet all of the aforementioned effectiveness, durability and safety, researchers have been exploring the use of natural substances in treating and producing textile products with antimicrobial properties. The antimicrobial activity of natural dyes (Gupta, Khare, & Laha, 2004; Joshi, Ali, Purwar, & Rajendran, 2009) on textiles has been discussed in literature. The effect of various plant extracts on the bacteria has been studied by a number of researchers in the past (Da & ErdoUrul, 2003; ErdoUrul, 2002; Reddy, Jamil, Madhusudhan, Anjani, & Das, 2001). The antibacterial properties of neem oil in combination with other herbal oils such as clove, tulsi and karanga have been used to impart antimicrobial finish on cotton textiles (Joshi et al., 2009; Thilagavathi, Rajendrakumar, & Rajendran, 2005). Work on antimicrobial finishing of 100% cotton and PET/cotton blend fabric using neem seed extract has been recently reported by our group (Joshi, Ali, & Rajendran, 2007; Purwar, Mishra, & Joshi, 2008). Chitosan, a biopolymer derived from a component found in crustacean shells called chitin, has long been known to possess antimicrobial attributes. Antimicrobial textiles using chitosan is also extensively reported in the literature (Lee, Cho, & Cho, 1999; Seong, Kim, & Ko, 1999; Shin, Yoo, & Jang, 2001). Antimicrobial fibers obtained from chitosan are readily available in the market for potential use (Kumar, 1999; Nam, Kim, & Ko, 2001).

More recently researchers working in the area of textiles and polymers are investigating the possible applications of nanotechnology for producing more appealing and highly functional value-added textile/polymeric substrates. Coating the surface of textiles and clothing or incorporating the fibres with nanoparticles is the latest approach for the production of highly active textile surfaces with a range of functionality such as UV blocking, antimicrobial, flame retardant, water repellant and self-cleaning properties, etc. While antimicrobial properties are exerted by nano

* Corresponding author. Tel.: +91 11 26596623; fax: +91 11 26581103.
E-mail addresses: mangala@textile.iitd.ernet.in, mangalajoshi9@gmail.com (M. Joshi).

0144-8617/$ – see front matter © 2010 Elsevier Ltd. All rights reserved.
doi:10.1016/j.carbpol.2010.08.004

silver, several metal oxide nanoparticles such as nano TiO_2, ZnO, SiO_2, etc. as coatings impart self-cleaning and flame-retardant properties.

On the other hand, nano-biotechnology researchers are actively focused towards new technique of drug delivery through nanoparticles. The use of chitosan nanoparticle in protein and drug delivery system is being actively researched and reported in the literature (Kevin, Marie, Ana, Angels, & Maria, 2001; Xu & Du, 2003).

Although there is a lot of literature on use of chitosan based antimicrobial textiles where bulk chitosan has been used as coating or finishing (Joshi et al., 2009), but there is no systematic research carried out on characterization and the application of chitosan nanoparticles and silver loaded chitosan nanoparticles on polyester substrates to have enhanced antibacterial activity. Recently, Yang, Wang, Huang, and Hon (2010) studied the application of nanochitosan for wool fabric finishing where they showed the effect of molecular weight on the chitosan nanoparticle size and zeta potential and the effect of nanochitosan concentration on shrink-proof and antibacterial properties of the wool fabric. Moreover, most of the studies reported on chitosan nanoparticles for drug delivery or gene therapy application (Jayakumar et al., 2010; Kong et al., 2010).

This study aims to investigate the use of chitosan nanoparticles for antimicrobial textile applications as chitosan in nano form is highly active because of very high surface area to volume ratio and expected to have desirable bioactivity even at very low concentrations. Initially, a detailed physical, chemical and thermal properties of synthesized nanoparticles vis-à-vis bulk chitosan has been investigated. A comparative study has also been carried out to investigate the enhancement of bioactivity of nanochitosan treated polyester over the bulk chitosan finished polyester at the same concentration.

It is well-known that a single antimicrobial agent cannot work effectively against both the Gram-positive and Gram-negative bacteria and also a broad range of microbes. Chitosan shows antimicrobial activity on textile substrates at relatively high concentrations and does not show release property from the treated textiles for its medical application as sutures, bandages, etc. Silver is a known antimicrobial agent with a wide spectrum of activity. But, incorporation of silver nanoparticles on textile substrates has been challenge because of its low charge density. Therefore, for instance, silver nanoparticles are often encapped with poly(methacrylic acid) (PMA) to generate negative charge on the surface for attachment on nylon and silk fibres (Dubas, Kumlangdudsana, & Potiyaraj, 2006) which can reduce the antimicrobial efficacy of the silver particle as well. In the present case, chitosan acts as a stabilizing agent and prevent the oxidation of silver which forms black color on the textile substrates by transforming silver to silver oxides.

Therefore, the synthesis of chitosan nanoparticles loaded with silver ion can also be investigated so as to be effective against a wide range of microbes with sustained release of silver ion over time. Also silver loaded in chitosan nanoparticle could be easily incorporated in the textile structure along with the chitosan nanoparticles without the need of the capping agents. Thus, the present work would be an attempt to synthesize chitosan nanoparticles and silver loaded chitosan nanoparticles and to integrate them on polyester fabric for imparting enhanced antibacterial property for a wide range of medical textile applications.

2. Experimental

2.1. Materials

Chitosan (with a molecular weight of 440 kDa and deacetylation degree of 82%) and sodium tripolyphosphate (TPP) in the form of powder were obtained from Sigma–Aldrich chemical Co. Ltd. Silver nitrate was purchased from Qualigen. Sodium hydroxide and glacial acetic acid were supplied by Ranbaxy, India. Nutrient broth (Merck), nutrient agar (Merck) and agar-agar (Merck) were used to carry out the antimicrobial testing. The deionized water was obtained from Millipore Milli-Q water purification system.

2.2. Synthesis of chitosan nanoparticles

Chitosan solution was prepared by dissolving purified chitosan with sonication in 1% (w/v) acetic acid solution until the solution was transparent. Once dissolved, the chitosan solution was diluted with deionized water to produce chitosan solution of concentration at 0.01% (w/v) with a solution pH of 6.0 (p*K*a value 6.5) which is the optimized chitosan solution pH to get highest antibacterial activity (Ali, Joshi, & Rajendran, 2010). Sodium tripolyphosphate (TPP) was dissolved in deionized water at the concentration of 0.1% (w/v). Then TPP solution was poured drop wise to the chitosan solution under magnetic stirring at 1000 rpm using stirring bar. Then the mixture was stirred for additional 15 min. The formation of chitosan–TPP nanoparticles started spontaneously via the TPP initiated ionic gelation mechanism. The nanoparticles were formed at selected chitosan to TPP weight ratio of 5:1 at temperature of 25 °C (which is the optimized ratio to get optimum antibacterial efficacy as reported in our earlier work) (Ali, Joshi, & Rajendran, in press). Silver loaded chitosan nanoparticles were obtained by adding a solution of 1 mM silver nitrate ($AgNO_3$) to the chitosan nanoparticle suspension during chitosan nanoparticle synthesis before centrifugation and was stirred for another 1 h. The nanoparticles were separated by centrifugation at 9000 rpm for 45 min. Then the supernatants were discarded. Nanoparticles were extensively rinsed with distilled water. After centrifugation the chitosan nanoparticles were freeze dried by LABCONCO Freeze Dry System (FREEZONE 4.5) at −47 °C under 85×10^{-3} Mbar pressure before further use or analysis.

2.3. Colloidal titration

The extent of cross-linking or the residual cationic amino groups on the surface of nanoparticles were determined by colloidal titration based on the reaction between positively charged polyelectrolytes (chitosan solution or chitosan nanoparticle dispersion) and negatively charged polyelectrolytes (poly(vinyl sulfate kalium salt) (PVSK)) (average Mw ~ 170,000) (Kwon, Park, Chung, Kwon, & Jeong, 2003).

5 ml of chitosan solution or nanoparticle suspension was mixed with 100 μl of 0.2% toluidine blue indicator and titrated with 0.01 mmol/l PVSK standard solution until reaching the color transition, which was from blue to violet. Another 5 ml of double distilled water was taken to make blank assay. The amount of amino groups was calculated from the net consumed volume of PVSK standard solution (an average of at least three titrations) using the following equation (Musyanovych, Rossmanith, Tontsch, & Landfester, 2007):

$$\frac{\text{amino groups}}{\text{g chitosan solution or nanoparticle suspension}} = \frac{\Delta V M N_A}{SC} \quad (1)$$

where ΔV is the net consumed volume of PVSK in l, M is the molar concentration of PVSK in mol/l, N_A is Avogadro's constant (6.023×10^{23} mol/l) and SC is the solid content of chitosan or chitosan nanoparticles in g.

The ratio of residual amino groups (RRAGs) on the surface of the chitosan nanoparticles was calculated with the following

equation:

$$\text{RRAG\%} = \frac{\text{residual amino groups per gram of chitosan nanosuspension after cross-linking}}{\text{total amino groups per gram of chitosan solution before cross-linking}} \times 100 \quad (2)$$

2.4. Characterization of chitosan nanoparticles

2.4.1. Hydrodynamic size and zeta potential of the synthesized chitosan nanoparticles

The size and zeta potential of the nanoparticles suspension was measured by The Delsa™Nano C (Beckman Coulter, USA) Particle Analyzer. Dynamic light scattering (DLS) also known as photon correlation spectroscopy (PCS) was used to measure the hydrodynamic diameter and size distribution (polydispersity index). All DLS measurements were done with a wavelength of 658 nm (with 2 Laser diodes, 30 mW) at 25 °C with an angle of detection of 165°.

PCS makes it possible to calculate the average diffusion coefficient (D) of the particles. Assuming that the particles are solid, the mean diameter (d) can be easily calculated by the Stokes–Einstein equation,

$$d = \frac{kT}{3\pi\eta D} \quad (3)$$

where k is the Boltzmann constant, T is the absolute temperature, and η is the viscosity of the medium.

Zeta potential of the nanoparticles suspension was measured by electrophoresis which refers to movement of charged particles in a fluid when an electric field is applied. Electrophoretic mobility is determined from the Doppler shift by using a non-invasive and quick technique called electrophoretic light scattering (ELS). The zeta potential of the suspension was measured with an angle of 15° at 25 °C.

2.4.2. Fourier transform infrared (FTIR) measurements

Infrared spectroscopy (IR) of chitosan, chiosan nanoparticle and silver loaded chitosan nanoparticle were carried out in pellet form, made from a small sample (7.0–9.0 mg) and KBr (45 mg) using 400 kg/cm^2 pressure for 10 min, on a PerkinElmer BX II FTIR spectrometer. All the data were taken in transmittance mode.

2.4.3. X-ray diffraction (XRD) pattern

X-ray powder diffraction patterns of chitosan, chitosan nanoparticles and silver loaded chitosan nanoparticle were obtained by a Phillips X-PERT PRO X-ray machine. The X-ray source was Cu Kα radiation (40 kV, 80 mA). Samples were scanned at a scanning rate of 4° min^{-1}.

2.4.4. Differential scanning calorimetry (DSC)

DSC scans were recorded using a differential scanning calorimeter (PerkinElmer Model DSC 7). Three milligrams of the samples were accurately weighed into aluminum pans without seals and heated from 50 to 380 °C at a heating rate of 20 °C/min under a nitrogen flow pressure of 40 ppsi.

2.4.5. Thermogravimetric analysis (TGA)

TG analysis was performed with a PerkinElmer TAC 7/DX TG analyzer. The mass of each sample was 5 mg. The carrier gas was nitrogen with a sample purging pressure of 2.6 kg cm^{-2}. The samples were heated from 50 °C to 500 °C to record the TG curves.

2.4.6. Morphology study of the nanoparticles

The morphological characteristics (size and shape) of the nanoparticles were examined using a Transmission Electron Microscope (TEM) machine (Phillips C M 12). One drop of dilute chitosan–TPP nanoparticles dispersion was placed on a carbon coated 300 mesh copper grid with the help of a syringe and then allow to sit till air-dried. Then the sample was viewed under the TEM.

2.5. Application of nanoparticles on polyester fabric

2.5.1. Hydrolysis of polyester fabric

Polyester (PET) fabric was given a hot water wash and dried at room temperature to remove temporary surface finish. These samples were cut into pieces (12 in. × 12 in.) and conditioned at standard temperature and humidity (temperature: 20 ± 2 °C and RH: 65 ± 2%) for 24 h. They were then weighed and used for alkaline treatment. The fabric samples were treated with 20% (on the weight of fabric) caustic soda using liquor ratio of 1:40 for 30 min and at a temperature of 80 °C on a constant temperature water bath with stirring. Following the alkaline treatment, the samples were rinsed repeatedly with distilled water and neutralized with dilute acetic acid (3% on the weight of fabric). Finally, the samples were dried at room temperature.

Initial weight of the fabric: 10.928 g
Weight after hydrolysis: 10.74 g
Weight loss: 1.7%
Tensile strength retention: 94%

2.5.2. Application of bulk chitosan (CS), nano CS (CSN) and Ag-CSN on hydrolyzed PET

In exhaust method the PET fabric was kept in 0.2% (w/v) of chitosan solution, nanochitosan and silver loaded nanochitosan dispersion with a substrate and liquor ratio of 1:20. The time kept for exhaustion on the fabric was 45 min at 60 °C. After removal the finished fabrics were washed thoroughly with water.

2.6. Dyeing of the CS, CSN and Ag-CSN treated polyester fabric

Dyeing was carried out to evaluate the difference between the available cationically charged surface active group of polyester surface finished with both the bulk and nanoparticle of chitosan.

Dyeing of the treated PET fabric was carried out with negatively charged acid navy blue dye (1% on the weight of the fabric) for 45 min at dyeing bath pH of 5.0.

The amount of dye absorption was used as a measure of extent of available surface functional groups (–NH_3^+) and was determined using a reflectance spectrophotometer (Gretag Macbeth, Color Eye-7000-A). The instrument analyzes the light being reflected from the samples and produces an absorption spectrum. The ratio between the sorption coefficient (K) and the scattering coefficient (S) can be extracted from the Kubelka–Munk equation (Eq. (4)) where R is the reflectance of the fabric at 520 nm (λ_{max} for acid navy blue dye).

The K/S value is commonly used to represent the amount of dye fixed or dye content of textile substrates. The reflectance of the acid navy blue absorbed coated polyester textile was measured at 360–750 nm and the K/S values were determined from the reflectance measurements.

$$\frac{K}{S} = \frac{(1-R)^2}{2R} \quad (4)$$

where K/S is the ratio of absorption and scattering coefficient and R is the reflectance of the fabric.

Table 1
Size and zeta potential value of chitosan and silver loaded chitosan nanoparticles.

Sample	Size (nm) measured at pH 6.0	PDI	Zeta potential (mV) at pH 6.0	RRAG (%)	Antimicrobial activity (%) (conc. 0.0001%)
Chitosan nanoparticle	115.5 ± 0.6	0.211 ± 0.002	13.35 ± 0.5	32.2	36
Silver (1 mM) loaded chitosan nanoparticle	165.8 ± 1.5	0.342 ± 0.023	12.97 ± 0.3	19.6	49

2.7. Antimicrobial activity assessment

2.7.1. Minimum inhibitory concentration (MIC)

The lowest concentration of agent that inhibited the visible growth of bacteria is considered as the minimum inhibitory concentration (MIC value). The MIC value of chitosan nanoparticles and their complexes against Gram-positive bacteria was determined by modified colony counting method (AATCC-100). Different concentrations of CS (0.01–0.1%), CSN (0.01–0.04%) and Ag-CSN (0.0005–0.01%) were tested against the bacteria to determine the MIC value. All the materials were sterilized at standard conditions, i.e. 120 °C, 15 psi and for 30 min before use. In this method, the sample was placed in a sterilized flask containing Luria broth solution inoculated with 10 μl of test organisms and incubated at 37 °C for 24 h in a laboratory shaker at 200 rpm. After incubation the number of colony forming unit (CFU) was counted by using serial dilution method. The percent reduction in number of colonies for treated sample as compared to the control samples gives the antibacterial activity of the chitosan.

2.7.2. Antibacterial activity of treated textiles

The antibacterial activity of the bulk chitosan, nano chitosan and silver loaded nano chitosan treated PET samples was tested using parallel streak method (AATCC-147) as well as modified colony counting method (AATCC-100) against *Staphylococcus aureus* bacteria. In this parallel streak method, bacteria culture was transferred to the agar plate in the form of streaks by the help of wire-loop. Streaks of 1 cm apart from each other were made on the plate. Then the prepared fabric swatch (2 in. × 1 in.) was pressed on the streak inoculum. Then the plates were incubated at 37 °C for 24 h. After incubation, bacterial growth was observed underneath and around the specimen. In modified colony counting method, the fabric swatch (2 in. × 1 in.) was placed in a sterilized flask containing Luria broth (Hi-media) solution inoculated with 10 μl of test organisms and incubated at 37 °C for 24 h in a laboratory shaker at 200 rpm. After 24 h incubation, serial dilutions of the liquid were made in sterilized water. Dilution of 10^{-3}, 10^{-4}, 10^{-5} and 10^{-6} were used for colony counting method. 10 μl were spread on to the agar plate and plates were incubated at 37 °C for 24 h. After incubation bacterial colonies were counted. The percent reduction in number of colonies in chitosan (in their different) treated sample as compared to the untreated samples gives the antibacterial activity of the treated fabric.

$$\text{antimicrobial activity or \%reduction} = \frac{A - B}{A} \times 100$$

where A is the bacteria colonies (CFU/ml) of untreated fabric and B is the bacteria colonies of the treated fabric.

2.7.3. UV–vis absorption

The bacterial reduction by the treated samples was reaffirmed by measuring the UV–vis absorption (turbidity or optical density of the solution) of the broth solution (untreated and treated with chitosan in their different forms) because bacteria suspension absorbs in 600–610 nm. Therefore, higher bacterial growth will directly be reflected by higher absorption value at 610 nm wavelength.

3. Results and discussion

3.1. Hydrodynamic size and zeta potential of the synthesized nanoparticles

The chitosan nanoparticles were synthesized by ionic cross-linking of positively charged chitosan with negatively charged TPP. The average hydrodynamic diameter, size distribution and zeta potential was determined by particle size analyzer (Delsa Nano C, Beckman Coulter, USA). It is evident from Table 1 that both chitosan and silver loaded chitosan nanoparticles has polydispersity index, PDI < 0.5 but silver loaded chitosan nanoparticles has comparatively higher size with higher PDI than chitosan nanoparticles because of surface chelation of silver ions with chitosan nanoparticles. Also the ionic silver is attached with the chitosan nanoparticles via formation of coordinate bonds with lone pair electron of free amino group of chitosan nanoparticles. Further there is also a chance of ionic bond formation between negatively charged phosphate ions and positively charged Ag ions in the complexes. In addition, there is a possibility of conversion of some of the silver ion to silver nanoparticles as well. Here, chitosan itself acts as a stabilizing as well as reducing agent (Murugadoss & Chattopadhyay, 2008) resulting in the reddish yellow color formation of the silver loaded chitosan nanoparticles suspension, indicating formation of silver nanoparticles. The attachment of silver ion with free amino group is further confirmed by lower zeta potential value of the silver loaded chitosan nanoparticles and reaffirmed by the value using colloidal titration. The RRAG (%) is lower in silver (1 mM) loaded chitosan nanoparticles (Table 1) indicating the attachment of silver ion with the surface free amino group of chitosan nanoparticles. Although the average size of silver loaded chitosan nanoparticles is higher along with lower zeta potential value, the antimicrobial activity against *S. aureus* is still higher. This is due to the release of silver ion from silver loaded chitosan nanoparticles and combined activity of chitosan and silver nanoparticles.

3.2. Crystallographic assay

Crystallographic structure of chitosan, chitosan nanoparticles and silver loaded chitosan nanoparticles were determined by XRD and are presented in Fig. 1. There is a strong peak in the

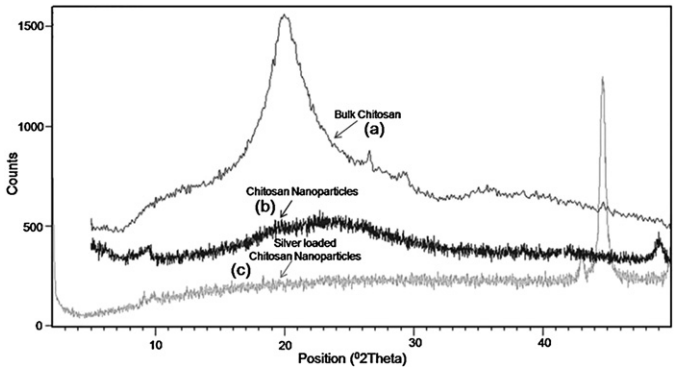

Fig. 1. XRD patterns of (a) chitosan, (b) chitosan nano (CSN) and (c) silver loaded CSN.

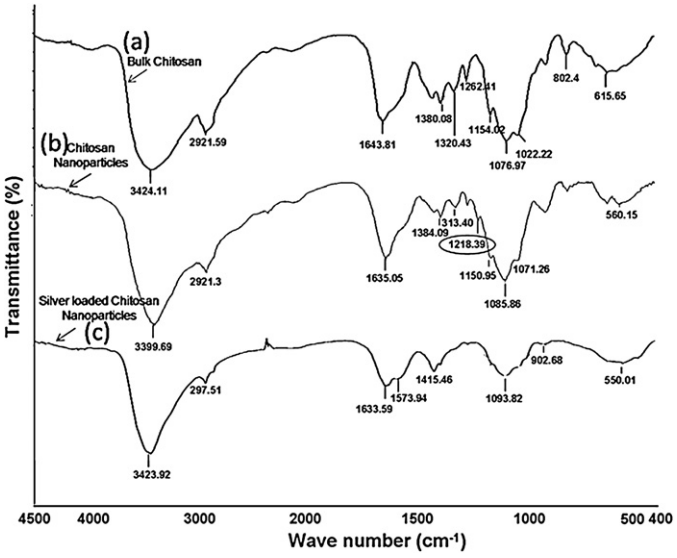

Fig. 2. FTIR spectra of (a) chitosan, (b) chitosan nanoparticle and (c) silver loaded chitosan nanoparticle.

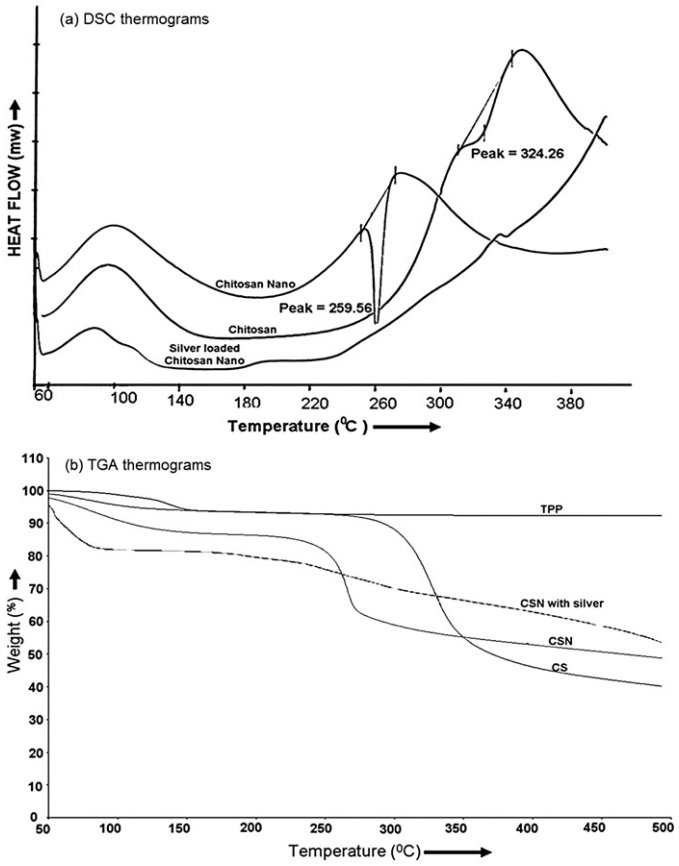

Fig. 3. Thermograms (a) DSC and (b) TGA.

diffractogram of chitosan at 2θ at 21.8°, indicating the high degree of crystallinity of chitosan, their crystal lattice constant α corresponding to 4.075. However, no peak is found in the diffractogram of chitosan nanoparticles. The XRD of chitosan nanoparticles is the characteristic of an amorphous structure. Chitosan nanoparticles are comprised of a dense network structure of interpenetrating polymer chains cross-linked to each other by TPP counter ions (Tang, Huang, & Lim, 2003). The XRD implicated greater disarray in chain alignment in the nanoparticles after cross-links. Silver loaded chitosan nanoparticle exhibits a sharp peak at 2θ at 44.3° which is due to the face centered cubic crystalline structure of silver, corresponding to crystal face of (2 0 0) silver (Cho & So, 2006).

3.3. Fourier transform infrared (FTIR) analysis

Chitosan nanoparticles were prepared by cross-linking of chitosan and tripolyphosphate (TPP). FTIR studies of chitosan and chitosan nanoparticles were performed to characterize the chemical structure of nanoparticles. FTIR spectra of chitosan and chitosan nanoparticles are shown in Fig. 2. A band at 3424.11 cm^{-1} indicates the combined peaks of the NH_2 and OH group stretching vibration in chitosan. In chitosan nanoparticles a shift from 3424.11 cm^{-1} to 3399.69 cm^{-1} is shown, and the peak of 3399.69 cm^{-1} becomes less wider, this indicates reduced hydrogen bonding. The reduced amount of hydrogen bonding in the cross-linked nanoparticle complexes is due to more open structure resulting from cross-linking with TPP. Whereas intense hydrogen bonding present in the compact bulk structure of chitosan leads to broadening of the OH peak. This finding is in disagreement with the finding obtained by Wu, Yang, Wang, Hu, and Fu (2005). In nanoparticles the peak of 1643.81 cm^{-1} disappears and a new sharp peak 1635.05 cm^{-1} appears. Also the intensity of amine bending at 1635.05 cm^{-1} goes down, which could be attributed to the linkage between tripolyphosphate group of TPP and ammonium group of chitosan nanoparticles. A new peak appears at 1218.39 cm^{-1} due to P=O stretching in chitosan nanoparticles which is absent in bulk chitosan. Binding of silver with N of the amine and amide group results in decreasing of intensity of amine and amide peaks at 1633.59 cm^{-1}. Division of combined peak of amine and amide at 1633.59 cm^{-1} and 1573.94 cm^{-1} also indicate the binding of Ag with O and N of those groups. The peak intensities in between 1000 cm^{-1} and 1350 cm^{-1} due to C–N stretching and bending is very less in silver loaded chitosan nanoparticles because of the complexation of chitosan with silver.

3.4. Thermal properties

Thermal properties of chitosan, chitosan nanoparticles and silver loaded chitosan nanoparticles were studied by DSC and TGA. In DSC curves (shown in Fig. 3a) the first peak of chitosan polymer at 66–130 °C exhibits endothermic peak attributed to the evaporation of absorbed and bound water. For chitosan nanoparticles and silver loaded chitosan nanoparticles the initial endothermic peak is due the loss of bound water. Differences in the peak area and the position of the first endothermic peaks clearly reveal the different water holding capacity of these macromolecules and different water–polymer interaction strength. Onset point of chitosan degradation starts at around 260 °C and reaches a maximum at around 340 °C with an exothermic peak at 324.26 °C (enthalpy, ΔH value −23.79 J/g). One prominent exothermic peak observed at around 260 °C temperature with onset temperature of 254.74 °C and peak temperature of 259.56 °C (enthalpy, ΔH value −79.76 J/g) is observed only for chitosan nanoparticles. This is probably due to the cleavage of the ionotropic interaction between the polycationic chitosan and polyanionic TPP. After that slow degradation continues but at a slow rate due to enhanced thermal stability because of the introduction of phosphorous (from the TPP of chitosan nanoparticles). In case of silver loaded chitosan nanoparticles a small endothermic peak in between 100 °C and 115 °C might be due glass transition temperature (T_g) of polymeric nanoparticles because of its complete amorphousness. Here, thermal degradation starts at around 230 °C but the rate and extent of degradation is very less unlike chitosan. One small exothermic peak found at around 340 °C is because of the presence of some uncrosslinked chi-

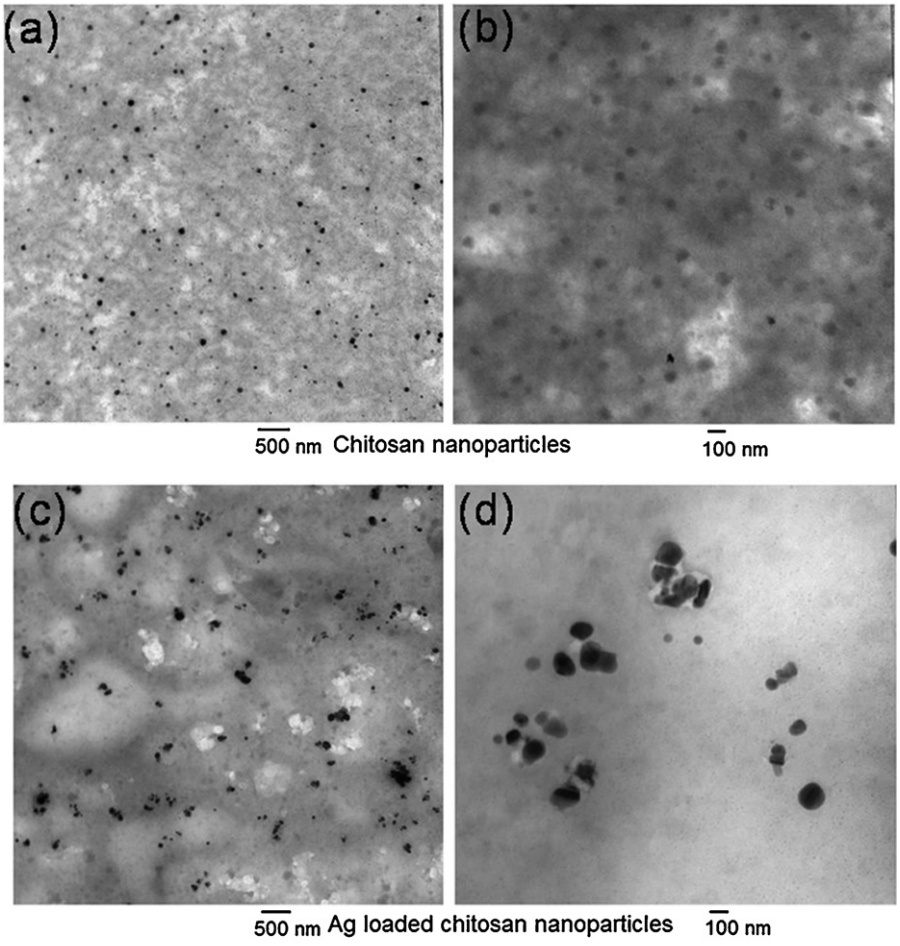

Fig. 4. TEM images of (a and b) chitosan nanoparticles (c and d) silver loaded chitosan nanoparticles.

tosan backbone. The introduction of silver in the polymer backbone has enhanced the thermal stability of the whole chitosan polymer backbone which was confirmed by the TGA studies as discussed below.

TGA of chitosan shows a weight loss in two stages shown in Fig. 3b. The first stage of weight loss about 6% in between 50 °C and 150 °C. This may be due to the loss of adsorbed and bound water. The second stage starts at 260 °C and continue up to 365 °C. In this region 46% weight loss happens due to degradation of chitosan. For chitosan nanoparticles the degradation behavior is somewhat like bulk chitosan. Here also the first stage of weight loss is due to the removal of moisture content and higher amount of water loss is due to the different arrangements of the molecular chains in the structure with higher amorphous domains and also due to the introduction of more polar group of TPP in the cross-linked backbones. In case of chitosan nanoparticles the onset degradation temperature starts earlier at around 210 °C and continues up to 270 °C because of its amorphous nature but it gains greater thermal stability than bulk chitosan up to the temperature range studied. The higher stability is due to the presence of inorganic phosphorous containing material in the cross-linked nanostructure. But in case of silver loaded chitosan nanoparticles the scenario is somewhat different which is as similar as DSC thermogram. Here more weight loss is there in the initial stages and the degradation starts at around 190 °C because of its complete amorphousness (also revealed in the XRD micrograph) and slow degradation continues up to the temperature range studied. The highest thermal stability for this sample among all the samples studied is due to the presence phosphorous as well as the silver both of which are inorganic in nature.

3.5. Morphology observation

The morphological characteristics of the chitosan–TPP nanoparticles were examined using the TEM technique. Fig. 4 reveals that the chitosan nanoparticles have spherical shape and a size range between 50 nm and 120 nm. The particles are well dispersed as well. On the other hand it also shows the image of silver loaded chitosan nanoparticles with a size range of 100–150 nm and an aggregate of distinctive single particles with clear joining boundaries formed which are spherical along with the regular geometry of the proximate polyhedron (pentagon and hexagon) shaped particles. The increased size and multishape formation is due to the attachment of silver on the chitosan nanoparticles to form a chelate like structure. The average size is smaller for both chitosan and silver loaded chitosan nanoparticles as compared to that measured by DLS system discussed earlier. This difference is due the measurement conditions used in the two techniques as well as the measuring technique and principle is different in two cases. In DLS the particles are dispersed in water media and are stayed in swelled condition and hydrodynamic diameter is measured in this system. On the other hand the particles are in dried stage on a TEM grid. Therefore, their structure is not in swelled stage resulting in lower size of the particles. In the TEM images of silver loaded chitosan nanoparticles aggregation with many distinctive single nanopar-

Table 2
Antimicrobial activity of solid chitosan (different form) against *Staphylococcus aureus* bacteria: determination of MIC value.

Samples	Concentration (%)	UV–vis absorption at 610 nm	Antimicrobial activity (%)
Control-I	–	2.2217	–
Control-II (150 ppm acetic acid)	–	1.9897	16
Bulk chitosan	0.01	2.2096	–
	0.02	1.4537	25
	0.04	0.8750	54
	0.10	0.0856	70
	0.50 (MIC)	0.0468	98
Chitosan nano	0.01 (MIC)	0.0615	92
	0.02	0.0541	100
	0.04	0.0093	100
Silver nitrate ($AgNO_3$)	0.00017	2.2057	–
	0.0017	0.6703	52
	0.017 (MIC)	0.0423	92
Ag-chitosan nano	0.0005	0.6545	40
	0.001 (MIC)	0.0210	94
	0.005	0.0056	100
	0.01	0.0059	100

ticles (each still possessing a similar nano-metric dimension) is observed.

3.6. Antimicrobial activity assessment

3.6.1. Minimum inhibitory concentration (MIC)

Minimum inhibitory concentration (MIC) given in Table 2 was found out against Gram-positive (*S. aureus*) bacteria. Here the different antimicrobial agents have been taken as a solid (powder) form. Preparation of true solution or suspension was avoided because the antibacterial agents ultimately will be present in the solid dry form on the polymer or textile substrates after application and drying. The solid chitosan in their different forms (bulk chitosan, nano chitosan, silver loaded nano chitosan) at different concentration levels has been dispersed directly in broth solution. Then this has been inoculated with 10 μl of test organism and is kept in shaker at 37 °C for 24 h. Inocula (10 μl) from this inoculated distilled water is spread over agar plate and incubated at 37 °C for 24 h. UV–vis absorption value of the inocula at 610 nm was also noted down. After incubation bacteria colonies (CFU/ml) were counted. Inoculated broth solution without any agent has been used as positive growth control-I and with 150 ppm acetic acid as control-II. MIC is determined as the lowest concentration of agent inhibiting the visible growth (more than 90% activity) of micro-

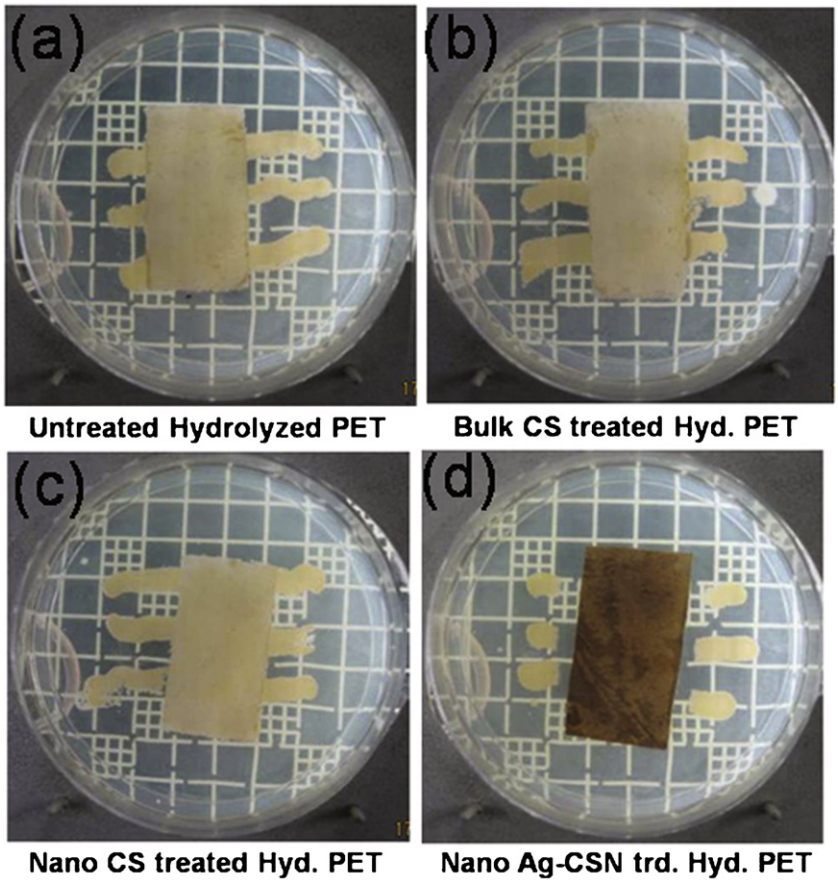

Fig. 5. Antibacterial activity (parallel streak method) of (a) untreated, (b) chitosan, (c) chitosan nanoparticle and (d) silver loaded chitosan nanoparticle treated PET fabric.

Table 3
Antimicrobial activity and dye uptake of treated PET fabric.

Samples	UV–vis absorbance at 610 nm	Antimicrobial activity (%)	'*K*/*S*' value with acid dye	Δ*E* value with respect to the undyed PET
Untreated polyester (PET)	2.5894	–	2.169	38.74
Bulk chitosan treated PET	1.7473	58	4.262	51.08
Nano chitosan treated PET	1.0336	90	6.748	58.81
Ag-CSN treated PET	0.0092	100	6.884	59.51

organism on the agar plate. The antimicrobial activity of silver nitrate salt (at different concentrations) was checked separately to explore the synergistic activity of silver and chitosan nanoparticle in the silver loaded chitosan nanoparticles form. An antimicrobial effect can be called as synergistic when the effects of two agents on the bacteria organism is greater than the effect of each individual agent, or the sum of the individual effect (i.e. the presence of one agent enhances the effects of second). It is clear from the Table 2 that silver loaded chitosan nanoparticle is exhibiting synergistic effect against *S. aureous* bacteria with very low concentration (0.001%, w/v) because at that concentration neither chitosan nanoparticles nor silver nitrate works effectively against the species tested.

3.6.2. Antimicrobial activity of CS, CSN and Ag-CSN treated polyester fabric

The antibacterial activity of chitosan, chitosan nanoparticles and silver loaded chitosan nanoparticles treated PET fabric was tested using parallel streak (AATCC-147) method using *S. aureus* bacteria. Bacterial growth underneath and around the cloth was observed. It is evident from Fig. 5 that both untreated and bulk chitosan treated PET fabric has experienced with yellowish bacterial growth to the edges of the fabric. Although there is no very clear zone of inhibition for nano chitosan treated PET fabric but bacterial growth is less at the edges and along the streaks. But in case of silver loaded chitosan nanoparticles treated fabric a very clear zone of inhibition is found. The very high antimicrobial activity of this fabric is due to the synergistic effect of silver and chitosan nanoparticles (as discussed earlier in MIC part) and a sustained release of silver ion with time. The higher antimicrobial activity of this fabric is also depicted in Table 3 where it shows very less UV–vis absorption at 610 nm wavelength with 100% reduction of bacteria with the concentration used.

The antibacterial activity of the treated fabric has also been evaluated quantitatively by AATCC-100 test method. It is evident from Table 3 that both chitosan (CS) and chitosan nanoparticles (CSN) treated PET show greater degree of bacterial reduction as compared to just the hydrolyzed PET. But CSN treated PET shows even more antibacterial activity than bulk chitosan treated fabric because of their enhanced surface area with higher number of available free amino groups to interact with the bacterial cell surface due to nano size of chitosan particles as indicated by the higher absorption of negatively charged acid dye (*K*/*S* value) by the chitosan nanoparticles treated PET fabric (Table 3). The higher value of color difference for (Δ*E*, with respect to undyed PET) nano chitosan treated PET as compared to bulk chitosan treated fabric also indicates the same. The antibacterial activity of the treated fabric was also reaffirmed by taking the absorbance of the broth solution (inoculated with both the bacteria and the PET fabric) at 610 nm. More reduction of bacteria for chitosan nanoparticles treated fabric is further reflected by the lower absorbance value of broth solution shown in Table 3.

4. Conclusions

This paper describes the preparation of novel chitosan nanoparticles and its application on bioactive polyester fabric to impart enhanced antimicrobial activity at a very low concentration. The nanoparticle is made by ionic gelation method using the biopolymer, i.e. chitosan (polycation) and a cross-linking agent, tripolyphosaphate (TPP) (polyanion). Cross-linking of chitosan with TPP was confirmed by FTIR. Amorphous characteristics of chitosan and silver loaded chitosan nanoparticle was revealed by X-ray diffraction pattern. The enhanced surface area with higher amount of available active amino group is also confirmed by higher dye uptake of negatively charged acid dye. The synthesized nanoparticles were found thermally more stable than bulk chitosan. Increased size and reduced zeta potential of silver loaded chitosan nanoparticles is a good indication of attachment of silver on the chitosan nanoparticles surface. The antimicrobial activity of chitosan gets much enhanced in nanoparticle form, as indicated by reduction in MIC from 0.5% to 0.01%. The silver loaded chitosan nanoparticle show a further increase in activity (MIC 0.001%) due to synergistic effect of Ag and chitosan nanoparticles. These particles additionally show a release mechanism as evident from a clear zone of inhibition. Both CSN and Ag-CSN treated polyester fabrics show acceptable antibacterial activity (90% and above) at very low concentration of 0.2% whereas the bulk chitosan gives only 58% activity at the same concentration.

Acknowledgements

We are grateful to the University of Bolton, UK for funding this research programme. One of the authors (S. Wazed Ali) is also grateful to the Commonwealth Scholarship Commission (Association of Commonwealth Universities), London, UK (Ref: INCN-2008-32) for awarding Split-Site Doctoral Fellowship-2008 tenable at UK and also like to thank British Council for making travel and financial arrangement to avail the scholarship at UK.

References

Ali, S. W., Joshi, M., & Rajendran, S. (2010). Modulation of size, shape and surface charge of chitosan nanoparticles with special reference to antimicrobial activity. *Advance Science Letters.*, *3*, 1–9.
Ali, S. W., Joshi, M., & Rajendran, S. (in press). Synthesis and characterization of chitosan nanoparticles with enhanced antimicrobial activity. *International Journal of Nanoscience*.
Cho, J. W., & So, J. H. (2006). Polyurethane–silver fibers prepared by infiltration and reduction of silver nitrate. *Materials Letters*, *60*, 2653–2656.
Da, A., & ErdoUrul, O. T. (2003). Antimicrobial activities of various medicinal and commercial plant extracts. *Turkish Journal Biology*, *27*, 157–162.
Dubas, S. T., Kumlangdudsana, P., & Potiyaraj, P. (2006). Layer-by-layer deposition of antimicrobial silver nanoparticles on textile fibers. *Colloids and Surfaces A: Physicochemical and Engineering Aspects*, *289*, 105–109.
ErdoUrul, O. T. (2002). Antibacterial activities of some plant extracts used in folk medicine. *Pharmaceutical Biology*, *40*, 269–273.
Gupta, D., Khare, S. K., & Laha, A. (2004). Antimicrobial properties of natural dyes against Gram-negative bacteria. *Coloration Technology*, *120*, 167–171.
Jayakumar, R., Chennazhi, K. P., Muzzarelli, R. A. A., Tamura, H., Nair, S. V., & Selvamurugan, N. (2010). Chitosan conjugated DNA nanoparticles in gene therapy. *Carbohydrate Polymers*, *79*, 1–8.
Joshi, M., Ali, S. W., Purwar, R., & Rajendran, S. (2009). Ecofriendly antimicrobial finishing of textiles using bioactive agents based on natural products. *Indian Journal of Fibre and Textile Research*, *34*, 295–304.
Joshi, M., Ali, S. W., & Rajendran, S. (2007). Antibacterial finishing of polyester/cotton blend fabrics using neem (Azadirachta Indica): A natural bioactive agent. *Journal of Applied Polymer Science*, *106*, 793–800.
Kevin, A. J., Marie, P. F., Ana, M., Angels, F., & Maria, J. A. (2001). Chitosan nanoparticles as delivery systems for doxorubicin. *Journal of Controlled Release*, *73*, 255–267.
Kong, X. Y., Li, X. Y., Wang, X. H., Liu, T. T., Gu, Y. C., Guo, G., et al. (2010). Synthesis and characterization of a novel MPEG–chitosan diblock copolymer and self-assembly of nanoparticles. *Carbohydrate Polymers*, *79*, 170–175.

Kumar, M. N. V. R. (1999). Chitin and chitosan fibres: A review. *Bulletin of Materials Science*, *22*, 905–915.

Kwon, S., Park, J. H., Chung, H., Kwon, I. C., & Jeong, S. Y. (2003). Physicochemical characteristics of self-assembled nanoparticles based on glycol chitosan bearing 5 h-cholanic acid. *Langmuir*, *19*, 10188–10193.

Lee, S., Cho, J. S., & Cho, G. (1999). Antimicrobial and blood repellent finishes for cotton and nonwoven fabrics based on chitosan and fluoropolymers. *Textile Research Journal*, *69*, 104–113.

Murugadoss, A., & Chattopadhyay, A. (2008). A 'green' chitosan–silver nanoparticle composite as a heterogeneous as well as microheterogeneous catalyst. *Nanotechnology*, *19*, 1–9, 015603.

Musyanovych, A., Rossmanith, R., Tontsch, C., & Landfester, K. (2007). Effect of hydrophilic comonomer and surfactant type on the colloidal stability and size distribution of carboxyl- and amino-functionalized polystyrene particles prepared by miniemulsion polymerization. *Langmuir*, *23*, 5367–5376.

Nam, C. W., Kim, Y. H., & Ko, S. W. (2001). Blend fibers of polyacrylonitrile and water-soluble chitosan derivative prepared from sodium thiocyanate solution. *Journal of Applied Polymer Science*, *82*, 1620–1629.

Purwar, R., & Joshi, M. (2004). Recent developments in antimicrobial finishing of textiles—a review. *AATCC Review*, *2*, 22–26.

Purwar, R., Mishra, P., & Joshi, M. (2008). Antibacterial finishing of cotton textiles using neem extract. *AATCC Review*, *8*, 35–44.

Reddy, P. S., Jamil, K., Madhusudhan, P., Anjani, G., & Das, B. (2001). Antibacterial activity of isolates from Piper longum and Taxus baccata. *Pharmaceutical Biology*, *39*, 236–238.

Seong, H. S., Kim, J. P., & Ko, S. W. (1999). Preparing chito-oligosaccharides as antimicrobial agents for cotton. *Textile Research Journal*, *69*, 483–489.

Shin, Y., Yoo, D. I., & Jang, J. (2001). Molecular weight effect on antimicrobial activity of chitosan treated cotton fabrics. *Journal Applied Polymer Science*, *80*, 2495–2501.

Tang, E. S. K., Huang, M., & Lim, L. Y. (2003). Ultrasonication of chitosan and chitosan nanoparticles. *International Journal of Pharmaceutics*, *265*, 103–114.

Thilagavathi, G., Rajendrakumar, K., & Rajendran, R. (2005). Development of eco-friendly antimicrobial textile finishes using herbs. *Indian Journal of Fibre and Textile Research*, *30*, 431–436.

Wu, Y., Yang, W., Wang, C., Hu, J., & Fu, S. (2005). Chitosan nanoparticles as a novel delivery system for ammonium glycyrrhizinate. *International Journal of Pharmaceutics*, *295*, 235–245.

Xu, Y. M., & Du, Y. M. (2003). Effect of molecular structure of chitosan on protein delivery properties of chitosan nanoparticle. *International Journal of Pharmaceutics*, *250*, 215–226.

Yang, H. C., Wang, W. H., Huang, K. S., & Hon, M. H. (2010). Preparation and application of nanochitosan to finishing treatment with anti-microbial and anti-shrinking properties. *Carbohydrate Polymers*, *79*, 176–179.